Journal of Advanced Scientific Research

Available online through http://www.sciensage.info

ISSN
0976-9595
Research Article

OPTIMIZATION OF RHODAMINE-B DYE SORPTION POTENTIAL FROM AQUEOUS SOLUTION USING ACTIVATED CARBON DEVELOPED FROM THE AERIAL ROOT OF *FICUS BENGHALENSIS L*

M. Kiruthiga[1], K. Ramesh*[1], A. Rajappa[2], K. Kamalakannan[3]
[1]*Department of Chemistry, Poompuhar college (Autonomous) (Affiliated to Bharathidasan University), Melaiyur, Nagapattinam - Dt. India*
[2]*Department of chemistry, Sri Manakula Vinayagar Engineering College, Madagadipet, Puducherry, India*
[3]*PG Assistant in Chemistry, SKSDS HigherSecondary school, Thirupanandal, Thanjavur Dt, India*
**Corresponding author: kr2467@gmail.com*

ABSTRACT

Adsorptive interaction of Rhodamine-B dye onto microwave assisted zinc chloride activated carbon from aqueous solution was investigated. Activated carbon was prepared from the aerial root of *Ficus benghalensis L.* Carbon prepared was designated as ZAC (zinc chloride activated carbon). Experiments were carried out in a batch process using various parameters such as pH, dose of the adsorbent, contact time, initial dye concentration. Kinetics of the system were studied with linearised forms of Lagergren, HO and Webber Morris model. Equilibrium data were showed with Langmuir, Freundlich, Tempkin, and Dubinin-Raduskevich isotherm equations. Implications obtained from the isotherm parameters were discussed. Thermodynamic parameters such as ΔH°, ΔS° and ΔG° were determined using Vant't Hoff plots. The XRD and FTIR spectral analysis were defined that adsorption was physisorption.

Keywords: Rhodamine-B, ZAC, isotherms, Kinetics, Thermodynamics, FTIR, XRD.

1. INTRODUCTION

One of the most important environmental problems faced the human in last and current century are the treatment of waste water due to increasing in industrial chemical effluents such as heavy metals, dyes, pigments, and other organic and inorganic chemical compounds discharge to water resources [1]. Dyes are largely abundant consisting hazardous water pollutant that has progressively threatened global peace. Dyes are venomous and non-biodegradable, their presence in the water even at very minute concentration pose mutagenic, teratogenic and carcinogenic effects on both aquatic life, humans and the ecosystem as a whole [2]. Many methods have been attempted to eliminate dyes from aqueous solution such as coagulation, filtration, precipitation, ozonation, adsorption, ion exchange and reverse osmosis [3]. Among these methods, adsorption is a widely applicable and superior technique owing to the low cost treatment and ease of design and operation. Many low cost adsorbents were prepared from waste materials such as coconut husk, date stone, almond shell, maize stem tissue [4, 5]. In this study we employed, the adsorbent obtained from the Aerial root of *Ficus benghalensis L* for the removal of Rhodamine-B from wastewater [6].

Rhodamine-B is synthesized organic dye used in paper, print, food, leather, pharmaceutical, cosmetic, laboratories as biological stain and so on. This dye has carcinogenic and toxic affect hence it's application in food and cosmetic is currently restricted [7].

The objectives of this study include the instrumental analysis such as FTIR, XRD and the investigations of the dye removal at different adsorbent dosage, Initial pH, dye initial concentration and contact time. Adsorption isotherm, kinetics and thermodynamics experiments were also investigated.

Nomenclature	
C_i	Liquid phase initial concentrations of the adsorbate (mg/L)
C_t	Liquid phase concentrations of the adsorbate at time "t" (mg/L)
C_e	Liquid phase concentrations of the adsorbate at equilibrium (mg/L)

V	Volume of adsorbate solution in liter (L)
W	Mass of the adsorbent (g)
q_e	Quantity adsorbed at equilibrium (mg/g)
q_t	Quantity adsorbed at time "t" (mg/g)
T	Time in minutes
Q_e	Amount of solute adsorbed per unit weight of adsorbent (mg/g)
C_e	Equilibrium concentration of solute in the bulk solution (mg/L)
Q_0	Langmuir adsorption efficiency
B	Langmuir adsorption energy
R_L	Langmuir separation factor
C_0	Initial concentration of the adsorbate
K_f and n	Freundlich constants incorporating all factors affecting the adsorption capacity and intensity of adsorption respectively
B_1	Tempkin constant related to heat of sorption (J/mol)
K_T	Tempkin equilibrium binding constant
q_D	D-R isotherm theoretical saturation capacity (mg/g)
B	D-R isotherm constant related to the mean free energy
E	D-R isotherm Polanyi potential
E	D-R isotherm mean free energy of adsorption
R	Gas constant
T	Temperature (K)
k_1	Rate constant of adsorption (1/min)
k_2	Second-order constants
H	Initial adsorption rate (mg/g min)
N	Number of data points

2. MATERIAL AND METHODS

2.1. Preparation of activated carbon

The aerial root of *Ficus benghalensis L* were cut into small portions and crushed in a pulveriser. About 20 g of the crushed roots was mixed with 75 mL of zinc chloride solution of desired concentration (20, 40 and 60%). The slurry was kept at room temperature for 24 hours. Then the slurry was subjected to microwave heating of pre-determined duration (8, 10, and 12 Minutes). Thus the carbonized samples were washed with 0.5 M HCl followed with hot distilled water and cold distilled water until the pH of the washings reach 7. Then the carbon was filtered and dried at 423K. The prepared carbon was designated as Zinc chloride Activated Carbon (ZAC) [8, 9].

2.2. Preparation of adsorbate solution

Analar grade Rhodamine-B dye was used for making the dye stock solution which was prepared by dissolving appropriate amount of accurately weighed dye in double distilled water to a concentration of 1000 mg/L. The experimental solutions were prepared from the stock solution by proper dilution.

2.3. Batch Adsorption experiments

The removal of Rh-B dye on ZAC was studied at various temperatures (305 K, 315 K and 325 K) using the batch technique to investigate the effects of operational parameters such as initial dye concentration, contact time, adsorbent dose, pH and solution temperatures. This is the process by changing one parameter at a time, while other parameters being kept constant. The adsorption process was carried out with three different initial concentrations at 25 mg/L, 50 mg/L and 75 mg/L of the dye. One g of adsorbent was taken in 250 mL iodine flask. 50 mL of the dye solution was added to the flask. This aliquot was shaken in rotary shaker at 180 rpm for predetermined time. Then the solution was centrifuged and the dye concentration of the centrifugate was measured using systronics double beam UV-Visible spectrophotometer: 2202 at 555nm to determine the percentage removal of the dye from the solution. The percentage of removal of dye was calculated using the following equation [10].

$$\text{Removal (\%)} = C_i - C_e / C_i \times 100$$

Where C_i is the initial concentration of the adsorbate (mg/L) and Ce is the concentration of the adsorbate at equilibrium (mg/L).

3. RESULTS AND DISCUSSION

3.1. Effect of adsorbent dosage

The adsorption studies of Rh-B dye onto ZAC was studied by varying the dose of the adsorbent from 10 to 100 mg. The percentage of removal of adsorbate from aqueous solution increased with an increase of carbon dose upto 30 mg after that removal percentage remains unchanged (Fig. 1). This trend is due to the increase in active sites for the adsorption of Rh-B with increasing adsorbent dosage. High adsorbent dosage results in little improvement in dye adsorbent. This may be due to higher collision rate between the adsorbent particles, resulting in less vacant sites per unit mass of adsorbent available for adsorption, and such collisions may lead to overlapping or aggregation of active sites. Hence, the amount of 30 mg was chosen as the optimised dosage of adsorbent and was used for the rest of the experiment [11].

3.2. Effect of Contact time

The effect of contact time on the removal of the Rh-B dye is shown in Fig.2. It is observed that initially the percentage removal of the dye increases rapidly and then increases in a slow and gradual manner till it reaches the equilibrium. This is because a large number of surface sites are available for adsorption at the initial stages and as the adsorption process continues the adsorption sites available decreases. There was no appreciable change in the adsorption percentage above 80min. Hence all the experiments were conducted for a period of 80 min [12].

3.3. Effect of Initial dye concentration

Fig.3 shows the initial dye concentration effect in the adsorption of Rh-B dye by ZAC. The data shows that the dye uptake increases and the percentage adsorption of Rh-B dye decreases with increase in initial dye concentration. This increase (16.13-42.75 mg/g) is a result of increase in the driving force, *i.e.* concentration gradient. However, the percentage adsorption of Rh-B dye on ZAC was decreased from 64.50 to 57%. Though an increase in dye uptake was observed, the decrease in percentage adsorption may be attributed to lack of sufficient surface area to accommodate much more dye available in the solution. The percentage adsorption at higher concentration levels shows a decreasing trend whereas the equilibrium uptake of Rh-B dye shows an opposite trend. At lower concentrations, all Rh-B dye present in solution could interact with the binding sites and thus the percentage adsorption was higher than those at higher dye concentrations. At higher concentrations, lower adsorption yield is due to the saturation of adsorption sites. As a result, the purification yield can be increased by diluting the wastewaters containing high dye concentrations [13].

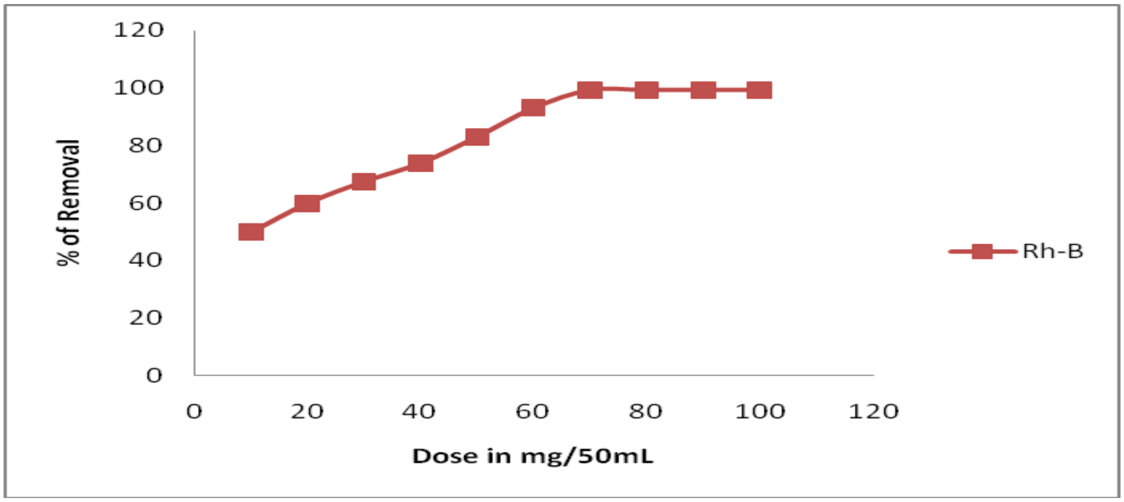

Fig. 1: Effect of Dose for Rh-B dye onto ZAC

Table 1: Percentage of Removal of dye and amount of dye adsorbed

Cimg/L	% of Removal of dye at equilibrium	Adsorbed amount of Rh-B dye at equilibrium (mg/g)
25	64.50	16.13
50	61	30.50
75	57	42.75

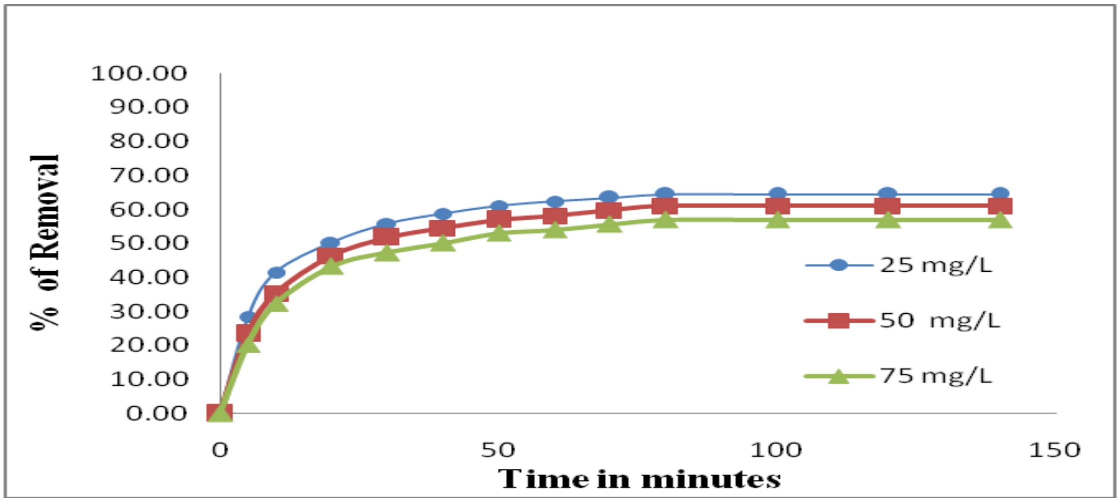

Fig. 2: Effect of contact time for Rh-B Dye onto ZAC

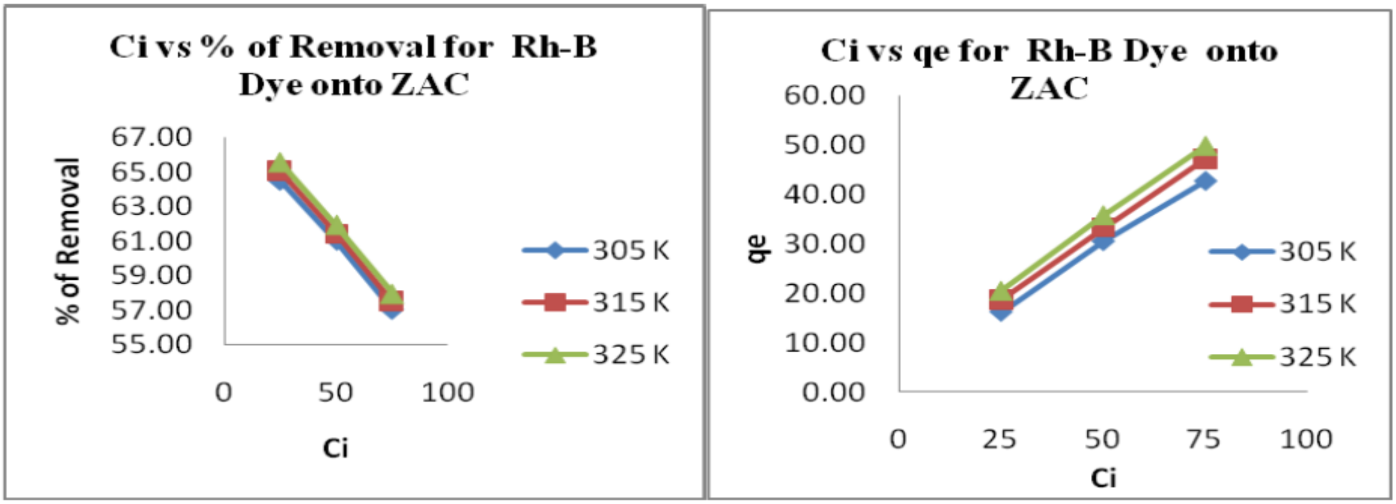

Fig. 3: Effect of Initial dye concentration for Rh-B dye onto ZAC

3.4. Effect of pH

The effect of pH on the uptake of Rh-B dye onto ZAC was investigated and the highest percentage of Rh-B dye adsorbed was obtained at pH 3 (fig 4). A gradual decrease was observed at above pH 3. The lowest amount of Rh-B dye adsorbed was at pH 11 (fig 4). At pH value of 3, Rh-B dye are of cationic and monomeric molecular forms, thus the dye molecule can enter easily into the pore structure of ZAC [14]. At pH value higher than pH zpc, the zwitter-ionic forms of Rh-B dye exist in solution mixture. This form increases the aggregation of Rh-B dye molecule to form larger molecules (dimers). The increase in aggregation of the zwitter ionic form is due to the attractive electrostatic interactions between the carboxyl and xanthene groups of the monomers. These molecules are unable to enter the pores as a result of their size thereby resulting in lower percentage removal at high pH [15].

3.5. Effect of Temperature

Fig 5 showed that the percentage of removal increased rapidly from 305, 315 and 325 K. An increase in the temperature definitely have pronounce effects of equilibrium capacity of Rh-B dye thereby increasing the amount of Rh-B dye molecule to sufficiently acquire energy to undergo interactions with the ZAC active site. There by the mobility of Rh-B dye molecules increased across ZAC external layers and within its internal pores. This further increases the formation of superior affinity existing between ZAC active site and the Rh-B dye. The qe (mg/g) of the ZAC progresses rapidly with increase in temperatures (*i.e.* 305K-325K).Temperature increase is also famous for enhancing the diffusion rate [16].

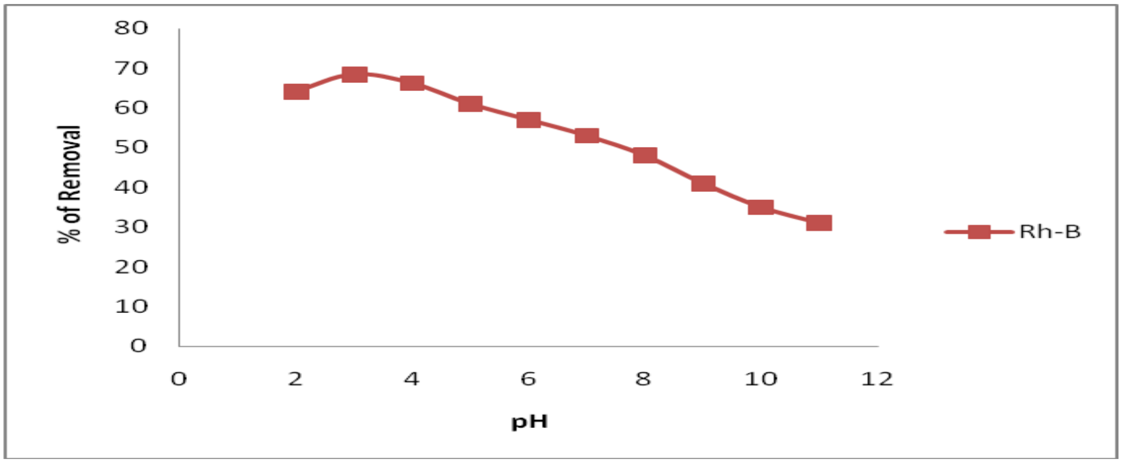

Fig. 4: Effect of pH on Rh-B dye onto ZAC

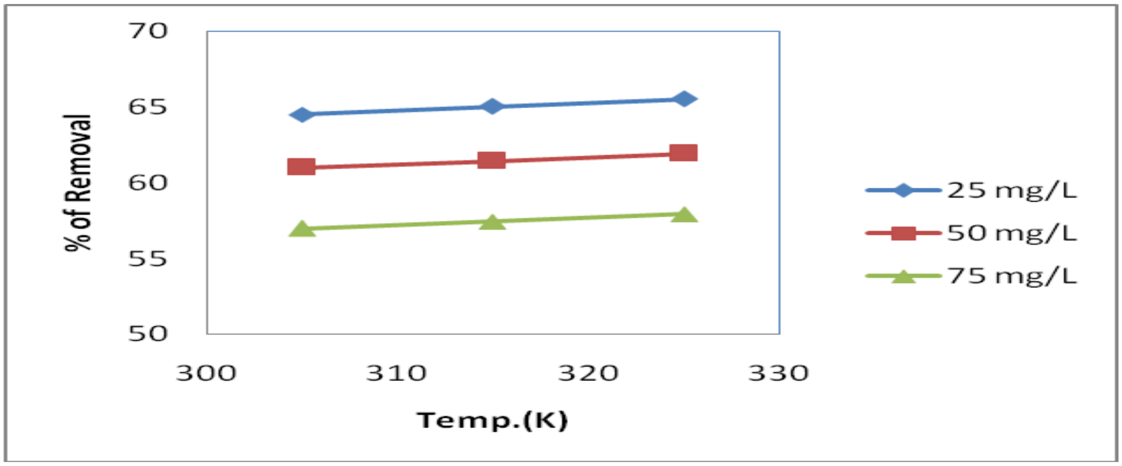

Fig. 5: Effect of Temperature for Rh-B dye onto ZAC

Table 2: Data Processing Tools

S. No.	Parameters		Formulae
1.	**Kinetic Models & SSE%**	Pseudo First order kinetics (Legergren equation)	$\log(q_e-q_t)=\log q_e-k_1/2.303\times t$
		Pseudo Second order kinetics (Ho equation)	t/qt =1/k2.qe2 +1/qe t
		The initial adsorption rate h	$h=k_2q_e^2$
		Intra particle diffusion (Weber-Morris equation)	$q_t=k_pt^{1/2}+C$
		Sumo ferror squares	$SSE(\%)=\sqrt{}\sum[(q)_{exp}-(q)_{cal}]^2/N$ e e
2.	**Isotherms**	Langmuir Separation factor	$C_e/Q_e=1/Q_0b+C_e/Q_0$ $R_L= 1/(1+ bC_0)$
		Freundlich	$\log Q_e= \log K_f+1/n\log C_e$
		Tempkin	$q_e=RT/b_T\ln a_T + RT/b_T\ln C_e$
		Dubinin- Raduskevich, Polanyi potential Mean free energy of adsorption	$\ln q_e = \ln q_D - B\varepsilon^2\varepsilon=RT\ln(1+1/C_e)$ $E=1/(2B)^{½}$
3.	**Thermodynamic Parameters**	Standard Freeenergy Change	$\Delta G°=-RT\ln K_c$
		Van't Hoff equation	$\ln K_c=\Delta S°/R -\Delta H°/RT$

3.6. Adsorption Isotherm Studies

Adsorption isotherm is crucial in the design of adsorption systems in wastewater treatment as it provides insight into interaction between the adsorbate and adsorbent. The equilibrium data obtained for Rh-B onto ZAC was fitted to the Langmuir, Freundlich, Tempkin and Dubinin-Radushkevich isotherm models [17-20].

3.6.1. Langmuir Isotherm

The monolayer adsorption capacity Qe values (mg/g) for adsorption of Rh-B dye onto ZAC system the values ranged from 100.00 to 142.857. The adsorption capacity increased with the increase of temperature. The values of Langmuir constant 'b', the adsorption energy ranges from 0.016 to 0.035 for all the three systems. These values indicate that the apparent energy of sorption is less and guidelines out the probability of strong interaction between the solute and adsorption site. The dimensionless separation factor R_L value ranged from 0 to 1 indicates favorable adsorption of Rh-B dye onto ZAC.

3.6.2. Freundlich Isotherm

Freundlich isotherm is an empricial equation employed to describe the surface heterogeneity. This isotherm deals with the multilayer adsorption of the substance on the adsorbent. The freundlich adsorption capacity constant Kf (mg/g) values ranged from 3.0974 to 3.7670 mg/g. The n values lies between 1 and 10 for favourable adsorption. In the present study 'n' value ranges from 1.2837 to 1.3158 which indicates the favorable adsorption.

3.6.3. Tempkin Isotherm

The results obtained from Tempkin model for the removal of Rh-B dye onto ZAC. b_T, Tempkin constant is related to the heat of adsorption. This b_T value increased from 124.1807 to 135.5770 as the temperature of adsorption increased. I n our present study the Tempkin parameters a_T values ranged from 0.2424 to 0.4315. Lower value of a_T and b_T with respect to adsorption of Rh-B dye is an indication of physisorption rather than chemisorption. The R^2 value was low compared to Langmuir and Freundlich.

3.6.4. Dubinin-Raduskevich

The Dubinin-Raduskevich (D-R) isotherm is generally used to describe the sorption isotherms of single solute system. The activation energy E value ranges from 0.5112 to 0.5169 and adsorption capacity qD value from 644.7318 to 560.5170 indicates the physisorption. The R^2 value was very low when compared to other three isotherms. In general the fitting data in isotherm equation were in the following order Freundlich> Langmuir >Tempkin>Dubinin-Raduskevich.

Table 3: Results of various isotherms plots for the adsorption of Rh-B dye onto ZAC

	Langmuir						Freundlich		
Temp K)	Q_0 (mg/g)	b (L/mg)	R^2	RL			n	kf	R^2
				25 ppm	50 ppm	75ppm			
305	100.00	0.016	0.994	0.7142	0.6060	0.533	1.3158	3.0974	0.997
315	111.111	0.026	0.999	0.5555	0.4347	0.3636	1.3175	3.5727	0.999
325	142.857	0.035	0.999	0.4545	0.3389	0.2758	1.2837	3.7670	0.999

	D-R				Tempkin		
Temp (K)	qD (mg/g)	Bx10^{-4} (mol^2/J)	E (KJ/mol)	R^2	bT (J/mg)	aT (L/mg)	R^2
305	42.15338	3.7425	0.5169	0.957	124.1807	0.2424	0.993
315	44.3147	3.7921	0.5135	0.987	134.1921	0.3374	0.992
325	45.8929	3.8270	0.5112	0.996	135.5770	0.4315	0.993

3.7. Adsorption Kinetics

The controlling mechanism of the adsorption process was analyzed according to the mathematical expressions given in Eqs. The optimum operating conditions for designing the purpose and adsorption mechanism is dependent on the kinetics of adsorbate uptake. In order to understand the kinetics of Rh-B dye adsorption onto ZAC as an adsorbent, pseudo first order, pseudo second order and intra particle diffusion models are tested with the experimental data.

The kinetic plots are shown in fig. 7. From the data in table 4, it is clear that the qe experimental value show some deviation from the qe calculated, qe values obtained for pseudo-first-order model from the linear plots in fig.7, whereas, for pseudo-second-order model, qe, exp is in good agreement with qe, calvalues. Correlation coefficient (R^2) value is usually used to select the best fit. The adsorption kinetics of Rh-B dye fitted best to the pseudo-second order adsorption model with R^2 values higher than pseudo-first order as shown in table 4 confirming that the pseudo-second order rate kinetics described the adsorption data most.

Apart from the models, the intra particle diffusion (IPD) parameter was used to determine the mechanism and rate-controlling steps. The intraparticle diffusion phase which is a gradual adsorption stage referred as the rate determining step. Here, the phenomenon of penetration of Rh-B dye molecules into the inner layers of adsorbent occurs gradually. Therefore, the transition that occurred through phases reveals the fact that the Rh-B dye diffusion from macropores to microporous [21-23].

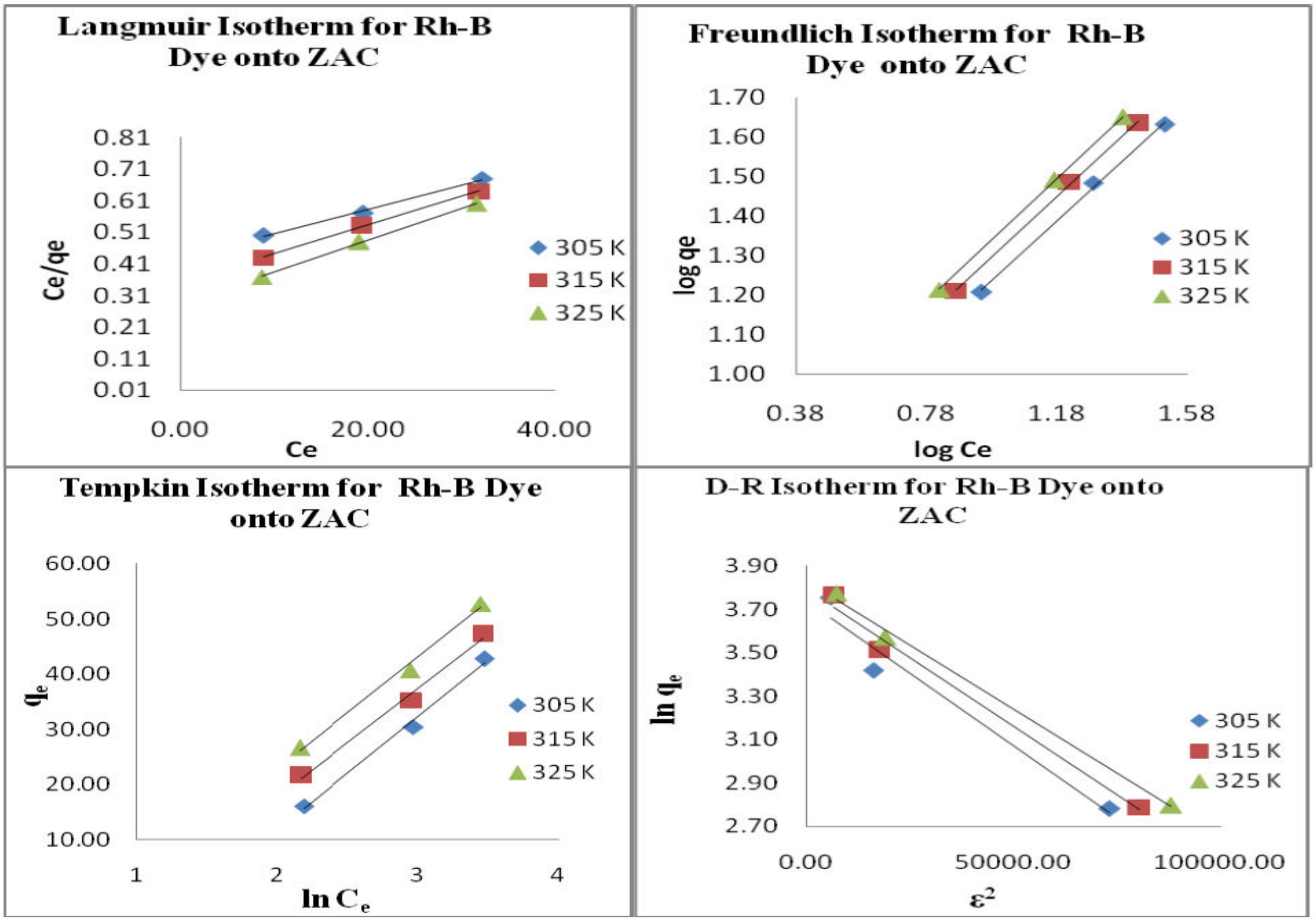

Fig. 6: Langmuir, Freundlich, Tempkin and D-R isotherms

Table 4: Kinetic parameters for the removal of Rh-B dye onto ZAC

C_i (mg/L)	First Order Kinetics					Second Order Kinetics					Intra Particle Diffusion	
	k_1 (min^{-1})	qe(cal) (mg/g)	Qe (exp) (mg/g)	R^2	SSE %	$k^2\times10^{-3}$ (g/mg.min)	qe(cal) (mg/g)	h	R^2	SSE %	kp(mg/ g.min)	R^2
25	0.0507	10.3753	16.95	0.986	5.49	0.0116	16.95	3.32	0.997	1.11	1.021	0.979
50	0.0461	21.2324	32.26	0.989		0.0049	32.26	5.13	0.996		2.012	0.981
75	0.0461	30.4089	45.45	0.985		0.0032	45.45	6.62	0.995		2.78	0.999

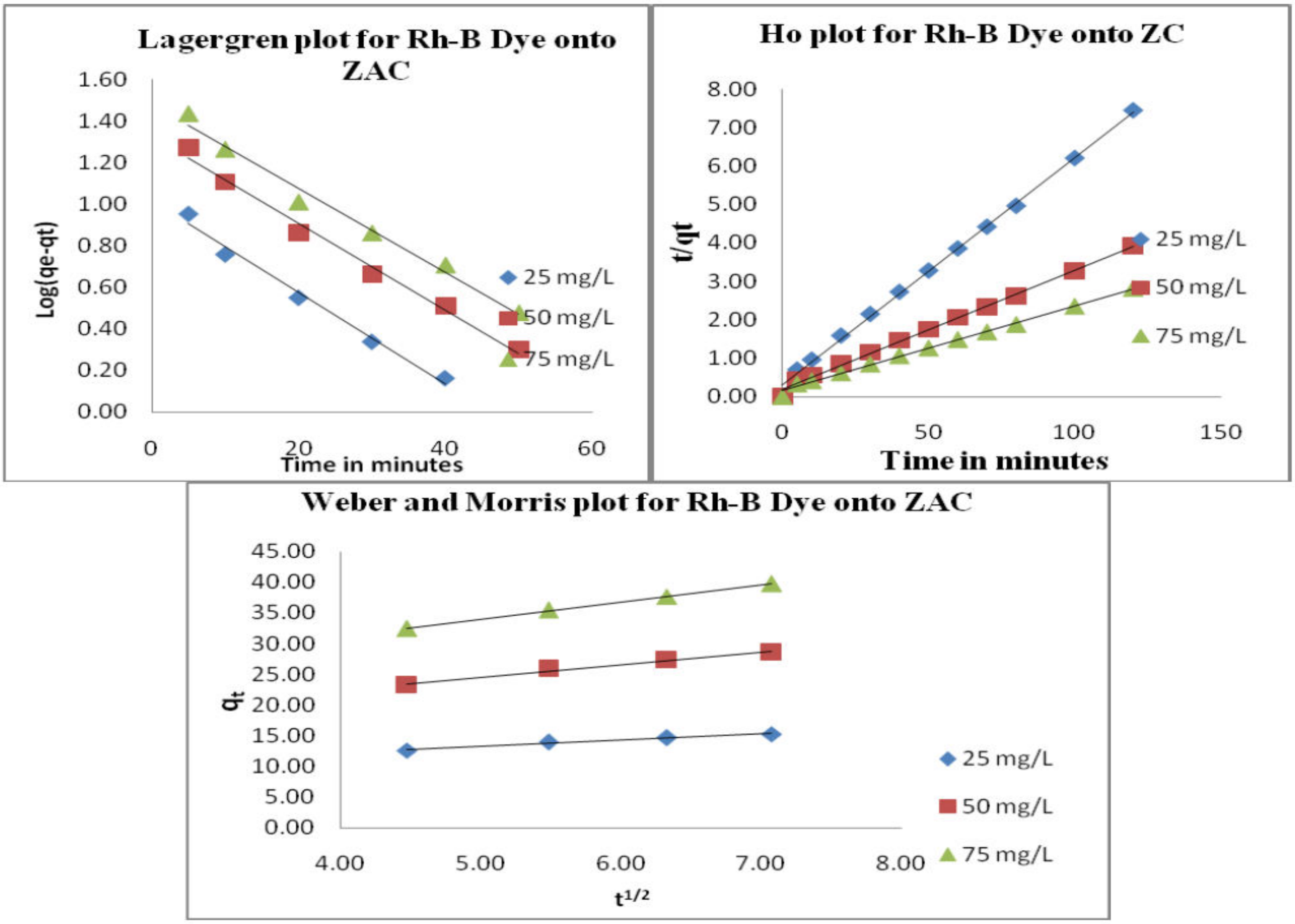

Fig. 7: Lagergren, Ho and Weber and Morris plot

3.8. Thermodynamic Study

These negative values represent spontaneous nature as well as feasibility of adsorption reaction. Decrease in ΔG° with the increase in temperature reflects better sorption at elevated temperature. Meanwhile, a plot of lnkd versus 1/T gives other thermodynamic parameters, namely, enthalpy and entropy changes of adsorption process. These values are shown in Table 5. Positive value of ΔH° indicates that the process is endothermic. Positive ΔS° indicated increased disorder of the dye molecules on the solid surface after adsorption. Low value of ΔH° also suggests that the adsorption may be due to physical binding forces [24].

3.9. Instrumental Analysis

Fig. 9 shows the FTIR spectra of Aerial root of *Ficus benghalensis* before (ZAC) and after activation (RZAC). Observations from Fig.9 showed a shift, broadening and disappearance of the peaks after activation of the adsorbent. The sharp intense band width at the region in between 3700-3926 cm^{-1} reveals that the presence of surface group such as carboxylic acids and hence asymmetric stretching of O-H is possible. Adsorption frequency is shifted from 3507cm^{-1} to 3550 cm^{-1} because of oxidative degradation and increase in temperature during the activation process infers the presence of phenolic hydroxyl groups [25]. The band at 2974cm^{-1} is ascribed to symmetric stretching vibration of C-H bond this is slightly shifted to 3022cm^{-1} in RZAC due to minute structural modification. Because of asymmetric C=N Stretching Vibration the peaks are obtained near 2200 cm^{-1}. But there is a inappreciable shift from 2259cm^{-1} to 2352 cm^{-1} in ZAC and RZAC respectively. Adsorption frequency at 1500cm^{-1} manifest that the presence of lactones surface group in the adsorbent and the C=O stretching vibrations are occurred at 1583cm^{-1} in ZAC and it is slightly shifted to 1596cm-1 in RZAC. These findings suggest that the decomposition of C-H bonds to form more stable aromatic C=C bonds at higher activation temperature [26]. The another consistent results is the absence of coupling band at 1876cm^{-1} is due to C=O symmetric stretching vibration for carboxylic acid derived from anhydrides. The bands at 1000cm^{-1} to 1100cm^{-1} may be due to stretching vibration of C-O group in alcohol phenol ether ester including carbonate group [27]. The peak near 700 cm^{-1} is probably due to Si-H stretching vibration of polycyclic and C-H bending vibrations of Benzene ring [28].

Table 5: Thermodynamic parameters for removal of Rh-B dye onto ZAC

Thermodynamic Parameters and their results					
Concentration (ppm)	**Temperature (K)**	**k_d**	**ΔG° kJ/mol**	**ΔH° kJ/mol**	**ΔS° kJ/mol**
25	305	1.8169	-1.5145	9.45	36.02
	315	2.0869	-1.9270		
	325	2.2844	-2.2326		
50	305	1.6154	-1.2163	10.04	36.91
	315	1.8309	-1.5824		
	325	2.1429	-2.0598		
75	305	1.3256	-0.7148	9.58	33.72
	315	1.4787	-1.0246		
	325	1.6729	-1.3906		

Table 6: FTIR Results for ZAC and Rh-B dye Loaded ZAC

Surface groups	Band Position cm^{-1}		Band Type
	ZAC	RZAC	
Carboxylic acid	3926	3869	O –H Asymmetric Stretching
	3779	3722	
Phenol	3507	3550	O –H Asymmetric Stretching
Carbon-Hydrogen	2974	3022	C –H Symmetric Stretching
	2259	2352	C = N Symmetric Stretching
Lactones	1583	1596	C = O Stretching Vibration
----	-----	1876	C = O Stretching Vibration
-----	1000-1100		C = O Stretching Vibration
-----	700		Si –H Stretching Vibration

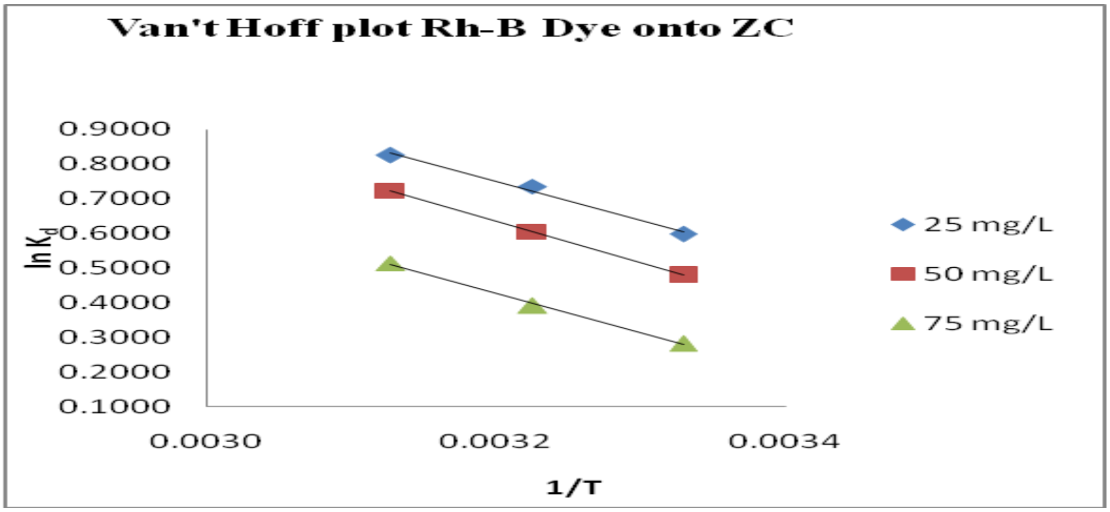

Fig. 8: Van't Hoff plot for Rh-B dye onto ZAC

3.10. XRD –Investigation

X-ray Diffraction technique is a powerful tool to analyze the ordered structure present in adsorbent. The result of XRD diffractograms of ZAC loaded with Rh-B dye suggested that the activated carbon may be amorphous in nature because it showed that the broad peak at around 2ϴ= 25° and also indicate that the adsorption process merely results very little change in surface structure of the adsorbent and adsorb mostly by physisorption [29-30].

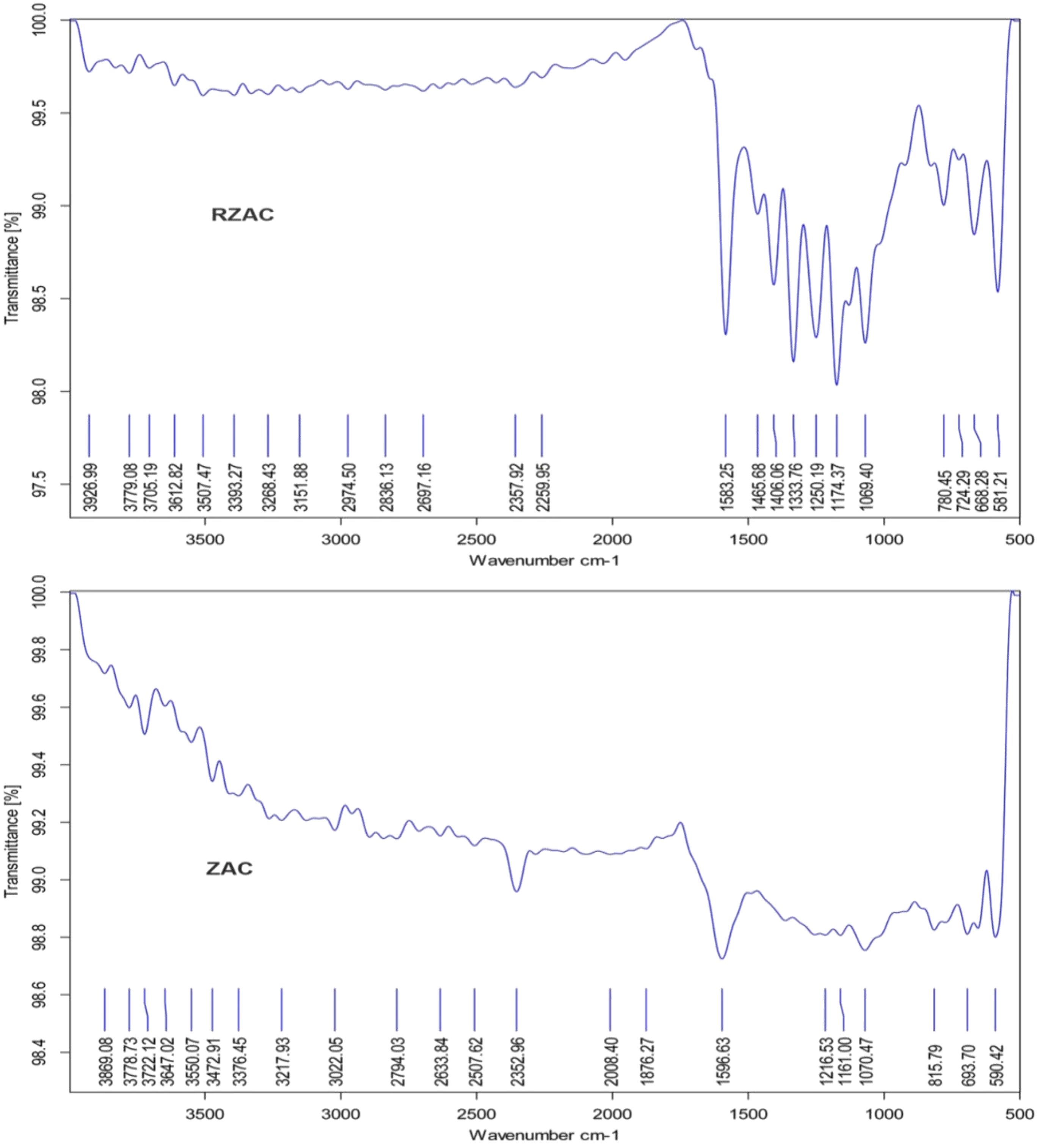

Fig. 9: FTIR before and after adsorption of Rh-B dye onto ZAC

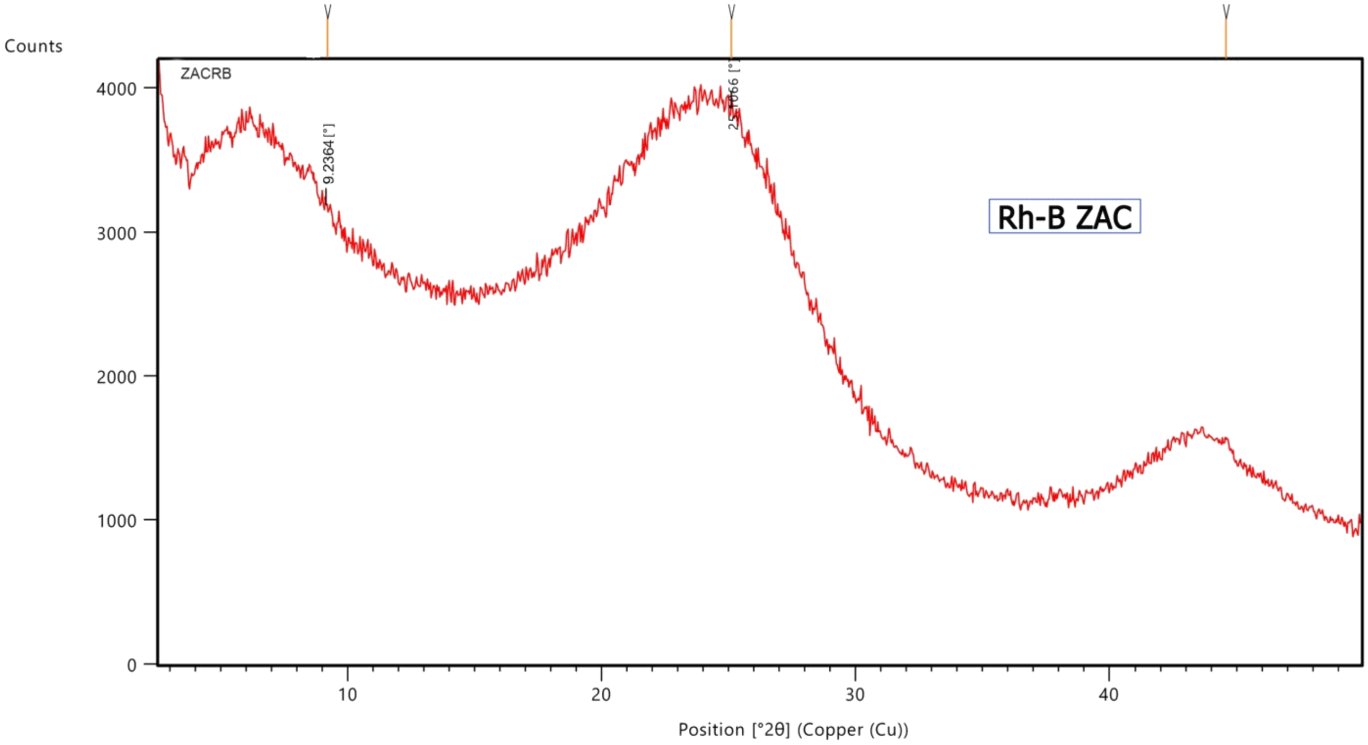

4. CONCLUSION

In the study, ZAC was successfully applied for the effective removal of Rh-B dye from aqueous solution making it as a potential, promising, sustainable and low cost adsorbent Analysis by XRD and FTIR spectroscopy revealed important adsorptive characteristics present in this novel adsorbent. Freundlich, Langmuir, D-R and Temkin isotherms were employed to fit the equilibrium data. The equilibrium adsorption data agreed reasonably well for Freundlich isotherm model. Adsorption dynamic study revealed that the adsorption process followed pseudo second-order equation. Surface adsorption and intra-particle diffusion were simultaneously occurring during the adsorption process and contribute to the adsorption mechanism. Thermodynamic studies shows that the adsorption process is spontaneous, endothermic and physisorption in nature.

Conflict of interest

None declared.

5. REFERENCES

1. Natarajan TS, Thomas M, et al. *Chemical Engineering Journal*, 2011; **169**:126-134.
2. Ahmad MA, Afandi KA, et al. *Appliedwater science*, 2015; **5**:407-423.
3. Jiang Y, Wu Y, et al. *Micro Chimica Acta,* 2008; **161(1-2):**137-142.
4. Klasson KT, Wartelle, et al. *Ind Crops Pro*, 2009; **30**:72-77.
5. Mohammadi M, Hassani AJ, et al. *Chem. Eng. Data J*, 2010; **55**:5777-5785.
6. Gupta VK, Pathania D. *Arian Journal of Chemistry*, 2017; **10**:2836-2844.
7. Barka N, Qourzals, et al. *Photochemistry and Photobiology Journal*, 2008; **195**:346-351.
8. Ramesh K, Rajappa A, et al. *Int. J. Res. Chem Environ*, 2014; **4(3)**:1-9.
9. Ramesh K, Rajappa A, et al. *Z.Phys. chem.*, 2017; **23(5)**:1057-1076.
10. Namasivayam C, Sangeetha D, et al. *J. Colloidal Interface Science*, 2004; **280**:359-365.
11. Nirmala S, Pasupathy A, et al. *Inter. J. Scientic Res*, 2016; **6(12)**:508-512.
12. Khudhair. A, Rudaini A, et al. *J. Al. Nahrain Uni*, 2017; **20(1)**:32-41.
13. Hemalatha K, Manivel A, et al. *Int. J. Biol. Chem,* 2018; **12**:1-7.
14. Bello OS, Lasisi BM, et al. *Chem. Speciat. Bio-available*, 2017; **29:**12-14.
15. Ojedokun AT, Bello OS, et al. *Appl. Water Science*, 2017; **7:**1965-1977.
16. Palanisamy PN, Agalya, et al, *Ind. J. Chemical Tech,*

2011; **20**:245-251.

17. Mittal A, Mittal J et al, *J. Colloidal. Interface Science*, 2010; **343(2)**:463-473.
18. Freundlich HMF. *Z. Phys. Chem*, 1906; **57A**:385-470.
19. Monika J, Garg et al, *J. Hazardous Material*, 2009; **162**: 365-372.
20. Gimbert F, Morin-Crini N, *J. Hazardous Material*, 2008; **157**:34-46.
21. Madhava Rao M, Ramana Dk, et al, *J. Hazardous Material*, 2009; **166**:1006-1013.
22. McKay G, Ho Ys, *Process Bio Chem,* 1999; **34**:451-465.
23. Weber WJ, Morris Jr et al, *J. Sanit. Eng. Div. ASCE,* 1963; **83(SA2):**31-59.
24. Li Q; Yue Q, et al, *J. Chem Eng,* 2010; **158**:489-497.
25. Khasri A, Bello O.S, et al. *Res.Chem. Intermed*, 2018; **44**:5737-5757.
26. Olugbenga Solomon B, Kayode et al. *J.Heliyon*, 2019; **5**:e02323.
27. Guliyane Felix de olivera et al. *Qium Nova*, 2017; **3(40)**:284-292.
28. Zhengfang Wang, Nie et al. *J.Eniviron sci pollut Res*, 2012; **19**:2908-2917.
29. Ramesh K,Rajappa et al, *Int.J.Curr.Res.Chem. Pharma. Sci* 2014; **11(4)**:15-19.
30. Li q,Yue Q, et al, *J.Chem Eng.* 2010; **158**:489-497.